

# High-resolution imaging of the OH megamaser emission in IRAS 12032+1707 and IRAS 14070+0525

Y. M. Pihlström<sup>1</sup>

*National Radio Astronomy Observatory, P.O. Box 0, Socorro, NM 87801*  
ypihlstr@nrao.edu

W. A. Baan<sup>2</sup>

*ASTRON, Oude Hoogeveensdijk 4, 7791 PD Dwingeloo, The Netherlands*

J. Darling<sup>3</sup>

*Carnegie Observatories, 813 Santa Barbara Street, Pasadena, CA 91101*  
and

H. -R. Klöckner<sup>2,4</sup>

*Kapteyn Institute, University of Groningen, P. O. Box 800, 9700 AV Groningen, The Netherlands*

## ABSTRACT

We present results from VLBA observations of the 1667 and 1665 MHz OH lines in two OH megamaser galaxies IRAS 12032+1707 and IRAS 14070+0525. For IRAS 12032+1707 we also present Arecibo HI absorption data. Almost all OH emission previously detected by single dish observations has been recovered in IRAS 12032+1707 and is found on a compact scale of <100 pc. The emission shows an ordered velocity field that is consistent with a single disk. However, the data is also consistent with a scenario including two physically different gas components. We explore this possibility, in which the two strongest and most blueshifted maser features are identified as the tangent points of a circumnuclear torus. The redshifted maser features would be extended in a direction perpendicular to the torus, which is in the direction of the merger companion. Thus, redshifted emission could be associated with an inflow triggered by a tidal interaction. HI absorption covers the velocities of the redshifted maser emission, suggesting a common origin. In the second source, IRAS 14070+0525, a large fraction of the OH emission is resolved out with the VLBA. We find no significant evidence of an ordered velocity field in this source, but these results are inconclusive due to a very low signal-to-noise ratio.

*Subject headings:* galaxies: individual (IRAS 14070+0525, IRAS 12032+1707) — galaxies: starburst — masers — galaxies: nuclei — radio lines: galaxies — techniques: interferometric

## 1. Introduction

Since the discovery of OH megamaser emission in Arp 220 (Baan et al. 1982), the detection of  $\sim 95$  OH megamaser have been reported (Baan et al. 1998; Darling and Giovanelli 2002; Martin et al. 1988; Staveley-Smith et al. 1987). These single

dish studies show that the shapes of the OH spectral lines are often complex, and cover velocities in the range  $10 \text{ km s}^{-1}$  up to a few  $1000 \text{ km s}^{-1}$  in each source.

Subsequent VLBI investigations of a few nearby OH megamaser galaxies, such as III Zw 35 and

Mrk 231, have demonstrated that the bulk of the OH maser emission arises in circumnuclear disks or tori (Pihlström et al. 2001; Klöckner et al. 2003). However, there are also indications that a single disk component cannot account for *all* maser emission, e.g. in Mrk 273; (Klöckner et al. 2004). Early single dish studies suggested the presence of blueshifted wings in several OH megamaser spectra (Baan, Haschick, and Henkel 1989). These have been interpreted as outflows, which possibly could provide an explanation for the emission that does not fit comfortably within a disk model.

The existence of outflows as well as inflows is not surprising, given that OH megamaser galaxies are exclusively associated with (Ultra)Luminous Infra-Red Galaxies ([U]LIRGs). (U)LIRGs probably represent short periods of nuclear starburst activity triggered by merger events. Such mergers will rapidly transport gas to the central regions, causing gas to fall inwards towards the nuclei. The combined effects of supernova explosions and stellar winds generated in this nuclear starburst can entrain the interstellar medium in outflows with velocities of 100 – 1000 km s<sup>-1</sup> (Heckman, Armus and Miley 1990; Alton, Davies and Bianchi 1999).

It is also possible that OH maser emission occurs in both of the merging nuclei, as has been seen in Arp 220 (Diamond et al. 1989). With a slight offset in systemic velocity between the two merging nuclei, the combined spectrum observed with a single dish telescope would be relatively broad. However, for the very broadest OH megamaser lines (exceeding 1000 km s<sup>-1</sup>), it is hard to interpret the lines either as originating from a single disk component or from a pair of nuclei. A combination of orbital mechanics, possible disk rotation, molecular inflow and outflow, and the velocity separation of the two main lines at 1667 MHz and 1665 MHz is likely to make up the velocity range in such OH megamaser spectra.

Earlier global VLBI experiments have reported the presence of 100 km s<sup>-1</sup> broad OH maser lines on parsec scales (Diamond et al. 1999). In this paper we will concentrate on investigating the cause of OH megamaser lines with widths exceeding 1000 km s<sup>-1</sup>. We report on VLBA observations of two OH megamaser galaxies, IRAS 14070+0525 and IRAS 12032+1707, that have full width zero intensity velocities of 1500 – 2000 km s<sup>-1</sup>. These objects are additionally interesting because of

their high redshifts ( $z = 0.217$  and  $z = 0.265$ ). Furthermore, their high OH luminosities of  $L_{\text{OH}} = 1.3 \times 10^4 L_{\odot}$  and  $L_{\text{OH}} = 1.2 \times 10^4 L_{\odot}$  respectively make the term 'gigamaser' suitable, and as such these galaxies are two of the most powerful OH megamaser galaxies known. The main aim of the current observations was to determine whether the broad lines are associated with inflows, outflows, rotating structures or violent kinematics. This paper also presents Arecibo H I absorption data for one of the sources, IRAS 12032+1707.

## 2. Observations

### 2.1. VLBA 1667/1665 MHz OH maser

IRAS 12032+1707 was observed in phase-referencing mode with the VLBA for 12 hours on 2002 July 8. The redshift of IRAS 12032+1707 ( $z = 0.217$ ) shifted the 1667.359 MHz line to 1369 MHz, that was used as the center of the observing band. To cover the complete OH emission velocity range of IRAS 12032+1707 ( $\sim 2000$  km s<sup>-1</sup>), a bandwidth of 16 MHz per left and right hand polarization was used. All telescopes were available at the time of the observations, and only minor periods of time required flagging due to radio frequency interference (RFI).

IRAS 14070+0525 was observed with a similar setup in June 9, 2002. The 16 MHz IF pair was centered on the redshifted ( $z = 0.265$ ) frequency of 1318 MHz. Due to RFI the KP telescope showed extreme and highly variable system temperatures, and to a large extent data had to be flagged for this telescope. Furthermore, the LA antenna was broken and so did not participate in these observations. At the observing frequency of 1318 MHz, several RFI spikes could be seen in the autocorrelation spectra. Since the frequencies at which these spikes occurred differed between the sites, they did not affect the cross correlation spectra for the most part. Badly affected time ranges were removed on 'by baseline' basis.

The data were correlated at the VLBA correlator in Socorro using the maximum 512 channels available. Data reduction was performed within AIPS. Both datasets were amplitude calibrated using the system temperature measurements, and fringe-fitting was performed on the phase-reference sources since the low signal to noise ratio (SNR) for the weak maser features

prevented self-calibration on any individual maser peak. For IRAS 12032+1707 the data were imaged using robust weighting, with a beam size  $11 \times 6$  mas ( $38 \times 21$  pc)<sup>1</sup>. IRAS 14070+0525 was imaged with natural weighting with a beam size of  $13 \times 6$  mas ( $53 \times 24$  pc)<sup>1</sup>. Before the cubes were analyzed, data were smoothed in frequency in order to further improve the SNR, to a channel increment of  $34 \text{ km s}^{-1}$  for IRAS 12032+1707 ( $1\sigma$  noise level per channel of  $0.6 \text{ mJy beam}^{-1}$ ) and  $82 \text{ km s}^{-1}$  for IRAS 14070+0525 ( $1\sigma$  noise level per channel of  $0.6 \text{ mJy beam}^{-1}$ ).

## 2.2. Arecibo 21cm HI absorption

To compare the velocity distribution of the OH emission with any possible HI absorption, data was taken at Arecibo on June 26, 2003. Observations were performed in position-switched mode with the L-wide receiver, covering a bandwidth of 12.5 MHz with 1024 spectral channels. Hanning smoothing was applied, and left and right polarizations were averaged to optimize the sensitivity. The total on-source integration time was 36 minutes, yielding an rms noise of 0.48 mJy.

## 3. Results

In order to determine the physical origin of the broad lines, we are interested in both the spatial distribution and the velocity fields of our sources. We present results of the data analysis for each source below.

### 3.1. IRAS 12032+1707 - OH emission

Figure 1 shows the spatial extent of OH megamaser emission in IRAS 12032+1707, averaged over all channels of signal above the  $3\sigma$  level. In addition to a central structure confined within a region of  $25 \times 25$  mas ( $\sim 87 \times 87$  pc), this map shows an extension of the source to the north-east. The maser line was too weak to perform self-calibration, and on larger scales than that shown in Fig. 1 we can see some weaker features in the map that are likely to be the results of calibration errors. The north-east extension is only seen at contours close to  $3\sigma$ , and it is uncertain

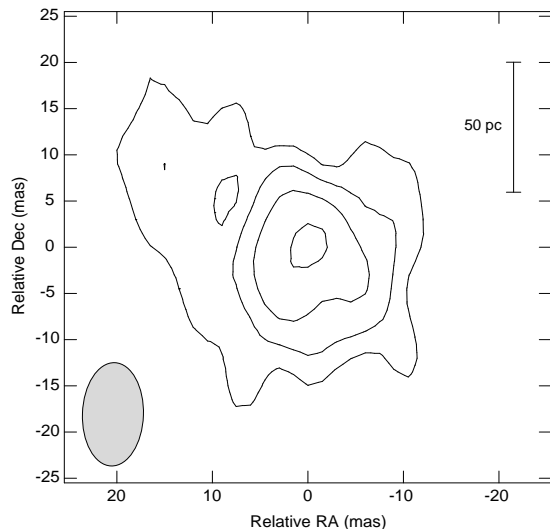


Fig. 1.— The OH maser emission distribution in IRAS 12032+1707, averaged over all channels with line emission. Contour levels are plotted starting at a  $3\sigma$  level of  $0.9 \text{ mJy/beam}$  and then increasing by a factor of  $\sqrt{2}$ . The beam size indicated in the lower left corner is  $11.3 \times 6.46$  mas. Given the SNR in our data, we do not consider the extension to the north-east as significant.

whether this feature is significant. Mapping the line emission at a few different resolutions, and using different weighting schemes show ambiguous results for this feature while the central component remains the same. Therefore we will not consider the north-east extension to be significant in the discussion in this paper.

We conclude that the OH maser emission is centered at RA 12:05:47.7225 and Dec 16:51:08.266 (J2000). This coincides, within the  $\sim 0.6''$  VLA positional errorbars, with the position given for the continuum in the NRAO VLA Sky Survey (NVSS, Condon et al. (1998)). Near-infrared (NIR) and optical imaging have identified two nuclei in this source (Veilleux et al. 2002) with a projected separation of  $3.8''$  (13.2 kpc) in an approximately north-south direction. From the NIR and the optical positions, we can thus associate all OH megamaser emission with the northern nucleus.

In Fig. 2 we plot the resulting spectrum including the emission in every pixel with emission

<sup>1</sup>Using  $H_0=71 \text{ km s}^{-1} \text{ Mpc}^{-1}$ ,  $\Omega_M = 0.27$  and  $\Omega_{\text{vac}} = 0.73$  in a flat universe, the linear scale is  $3.482 \text{ pc mas}^{-1}$  at  $z=0.217$  and  $4.046 \text{ pc mas}^{-1}$  at  $z=0.265$ .

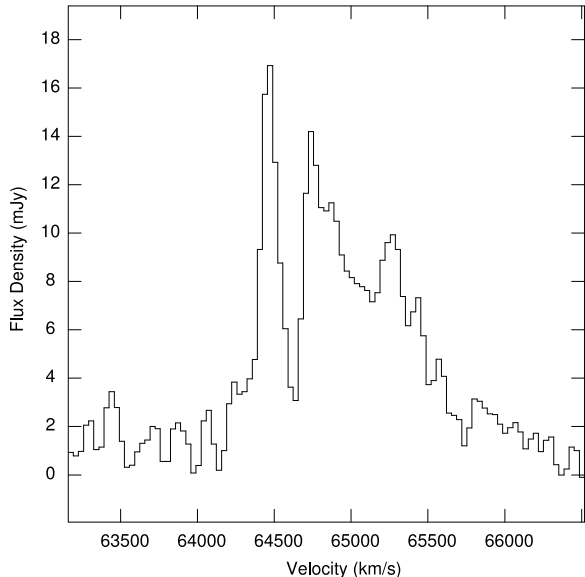


Fig. 2.— The total intensity spectrum of IRAS12032+1707. The flux density levels agree within the error bars to the flux density detected in earlier single dish spectrum. This indicates that we recover all emission in our VLBA data.

above  $3\sigma$ . The velocity scale is referenced to the 1667 MHz line, and the optical systemic velocity is  $65055 \text{ km s}^{-1}$  (Kim and Sanders 1998). This can be compared to the single dish spectrum published by Darling and Giovanelli (2001). Within the noise, we recover all of the single dish flux density in our VLBA data. There is a weak, redshifted wing at velocities above  $65700 \text{ km s}^{-1}$  in the spectrum by Darling and Giovanelli (2001) that is not clearly identified in our data. The  $3\sigma$  rms noise level in our spectrum is at  $1.8 \text{ mJy/beam}$ , which is at the same level as the emission in the Arecibo spectrum. Thus, we cannot determine whether the red wing is resolved out in the VLBA data, or whether it is hard to see because it is not discernible from the noise.

Since the SNR is limited in our data, we perform additional spectral averaging to extract velocity information from the cube. At least five peaks in our total intensity spectrum can readily be identified in the single dish spectrum. By averaging a range of six channels around each peak, we constructed five contour maps. 2-dimensional Gaussian fitting was then performed on each map to derive their centroid position. The positional

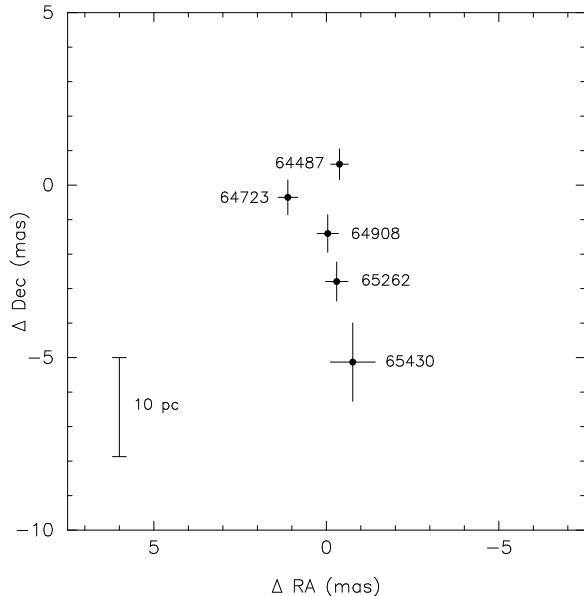


Fig. 3.— The spatial positions of the maser emission in IRAS 12032+1707. Each point represents a peak in the spectrum, and is plotted with  $1\sigma$  positional error bars.

error bars were calculated using the expression  $\sigma_{x,y} = \theta_{x,y}/(2 \text{ SNR})$  where  $\theta_{x,y}$  is the angular resolution in each direction, and the SNR is the SNR in each map. The result of the fitting is displayed in Fig. 3. Clearly there exists an ordered velocity field, with a major gradient seen in an approximately north-south direction.

The broad velocity extent of the OH emission implies the possibility of blending between hyperfine transitions at 1667 and 1665 MHz. In the heliocentric velocity frame these hyperfine lines are expected to have a velocity separation of  $428 \text{ km s}^{-1}$ . It could therefore be possible that the most blueshifted peak at  $64487 \text{ km s}^{-1}$  has its 1665 MHz counterpart in the peak at  $64908 \text{ km s}^{-1}$ . We note however that for the only cases in which the 1665 MHz emission has been detected in an VLBI experiment (Pihlström et al. 2001; Klöckner et al. 2004), the 1665 MHz emission closely follows the 1667 MHz distribution. Since the two peaks in our experiment have very different spatial positions, we will assume that the emission line is dominated by 1667 MHz emission. This is known to be the case for all OH megamasers with well separated hyperfine transitions.

### 3.2. IRAS 12032+1707 - continuum

From the NVSS IRAS 12032+1707 is expected to have a correlated 1.4 GHz continuum flux density of 29 mJy (Condon et al. 1998). Due to the broad line width of the OH maser emission, there was only a limited part of the observed band that contained line free channels. 20% of the total pass-band was selected and averaged in an attempt to search for the continuum emission. Using the same imaging parameters as described for the OH emission (Sect. 2.1) no significant continuum emission was detected at a  $3\sigma$  level of 0.3 mJy/beam. Given the beam size this implies that the continuum becomes resolved on scales less than around 75 mas (260 pc).

We note that using natural weighting, in combination with a heavy tapering of the data, yields a tentative detection of  $\sim 1$  mJy coincident with the location of OH emission. However, given that no self-calibration can be performed, the significance of this continuum emission is questionable. In future, more sensitive observations are required to address this issue.

### 3.3. IRAS 12032+1707 - H I

The Arecibo H I absorption spectrum is shown in Fig. 4. The H I absorption can be fitted by two Gaussian components with centroid velocities of 65119 and 65496  $\text{km s}^{-1}$  and full width half maxima of 186 and 166  $\text{km s}^{-1}$ , respectively. Overlaid on the H I spectrum is the VLBA OH maser spectrum (scaled down by a factor of 5 in amplitude), allowing a comparison between the H I and OH velocities. We conclude that the bulk of the H I absorption coincides in velocity with the reddest velocity components of the VLBA OH maser emission. The implied H I column densities can be estimated to  $N_{\text{HI}} > 5.5 \times 10^{20} \left(\frac{T_{\text{sp}}}{100\text{K}}\right) f^{-1} \text{ cm}^{-2}$ , where  $T_{\text{sp}}$  is the spin temperature and  $f$  is the filling factor.

### 3.4. IRAS 14070+0525 OH emission

Figure 5 shows the total integrated OH flux density that is recovered in our VLBA observations. As with IRAS 12032+1707, all velocity scales are referenced to the 1667 MHz line. The systemic velocity of  $79445 \pm 70 \text{ km s}^{-1}$  (Kim and Sanders 1998) is slightly offset from the velocity components detected in our VLBA data. We

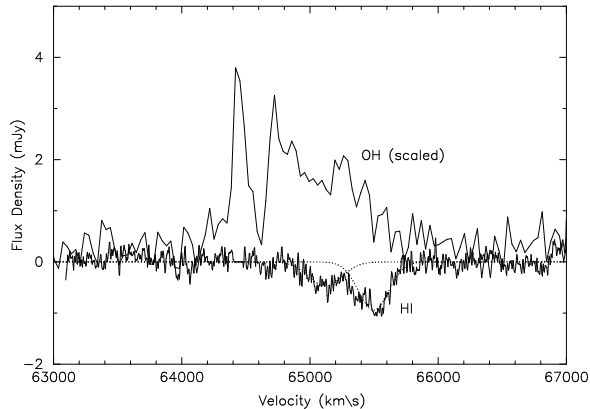


Fig. 4.— H I absorption spectrum (thick line) showing that the H I absorption in IRAS 12032+1707 corresponds to the reddest parts of the VLBA OH maser emission spectrum (thin line). The amplitude of the OH spectrum has been divided by a factor of 5, to allow a better comparison. In the H I spectrum a region around  $64450 \text{ km s}^{-1}$  has been blanked due to RFI.

can define two peaks in the spectrum, with corresponding velocity centroids of  $\sim 79900 \text{ km s}^{-1}$  and  $80250 \text{ km s}^{-1}$ . Given the low spectral resolution of our VLBA spectrum ( $82 \text{ km s}^{-1}$ ), these peaks coincide with peaks seen in the single dish spectrum at velocities of  $79950 \text{ km s}^{-1}$  and  $80200 \text{ km s}^{-1}$  (Baan et al. 1992). However, several distinct single dish peaks are missing from our VLBA spectrum, and we can only account for a minor part of the flux density observed by single dish ( $< 10\%$ ). For example, the single dish spectrum displays a prominent feature at around  $79000 \text{ km s}^{-1}$  that we do not detect. This implies that a large part of the emission is relatively diffuse. We note that these observations did not include LA and only partly the KP telescopes, leading to a substantial loss of the short baselines required to detect OH at angular scales  $> 80 \text{ mas}$  ( $> 325 \text{ pc}$ ).

Figure 6 displays the spatial extent of all emission detected, which is contained within a region of around  $10 \times 10 \text{ mas}$  ( $\sim 40 \times 40 \text{ pc}$ ). The emission is centered at RA 14 09 31.2446 and Dec 05 11 31.507 (J2000), which coincides with the optical and NIR nuclear positions reported by Kim et al. (2002).

Condon et al. (1998) measured a 1.4 GHz continuum flux density of 5 mJy. No continuum emis-

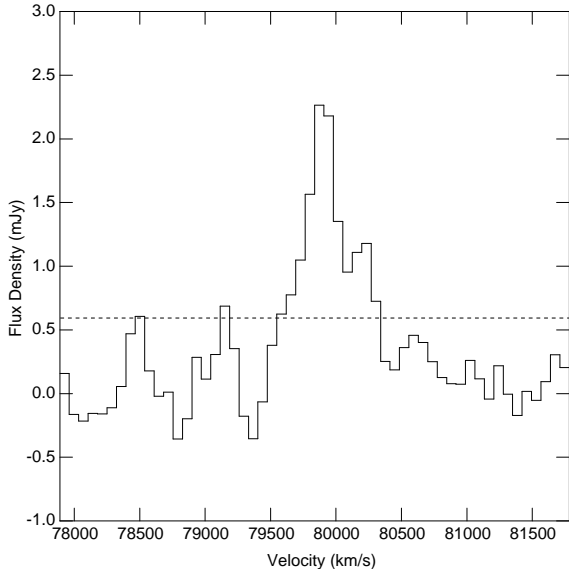


Fig. 5.— Total integrated OH maser emission in IRAS 14070+0525. The flux density is only a fraction of the flux density detected using a single dish. The dashed line across the spectrum shows the  $1\sigma$  noise limit.

sion was detected for IRAS 14070+0525 at a  $3\sigma$  level of 0.45 mJy/beam.

## 4. Discussion

### 4.1. IRAS 12032+1707 Continuum

The continuum in IRAS 12032+1707 is only tentatively detected at the shortest u,v distances (Sect. 3.2). In part, this result could be due to calibration errors, but it also indicates that the majority of continuum emission is found on scales larger than 260 pc (Sect. 3.2). That implies an upper limit of the brightness temperature to be around  $3 \times 10^6$  K. Such a brightness temperature and spatial distribution would be consistent with a starburst origin similar to that seen in Arp 220 (Smith et al. 1998) and III Zw 35 (Pihlström et al. 2001).

Many ULIRGs fall on the radio-FIR correlation for starbursts (Helou et al. 1985; Yun, Reddy and Condon 2001). This correlation can be understood by assuming that the radio emission is arising from starburst induced supernova remnants and from HII regions. Following the definitions

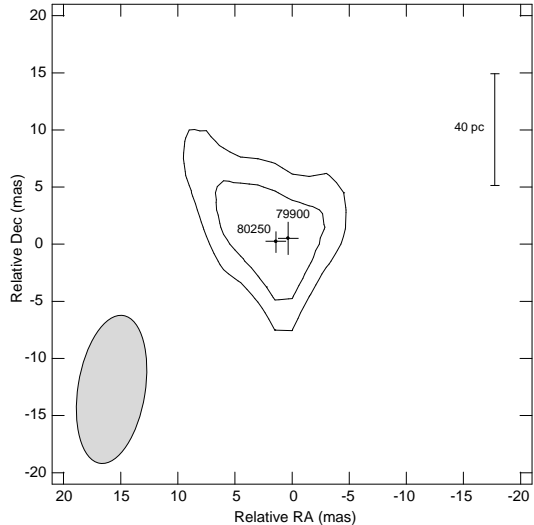


Fig. 6.— The OH maser emission distribution in IRAS 14070+0525, averaged over all channels with line emission. Contour levels are plotted starting at a  $3\sigma$  level of 1 mJy/beam and then increasing by a factor of  $\sqrt{2}$ . The beam size indicated in the lower left corner is  $13.01 \times 5.87$  mas. The two crosses mark the positions of the two peaks identified in the VLBA spectrum, shown with  $1\sigma$  error bars.

from Helou et al. (1985), the correlation is quantified by a logarithmic ratio between the far-infrared flux density ( $FIR$ ) and the 1.4 GHz radio flux density ( $S_{1.4\text{GHz}}$ ):

$$q = \log \left( \frac{FIR}{3.75 \times 10^{12} \text{Wm}^{-2}} \right) - \log \left( \frac{S_{1.4\text{GHz}}}{\text{Wm}^{-2}\text{Hz}^{-1}} \right) \quad (1)$$

where  $FIR$  is defined by

$$FIR = 1.26 \times 10^{-14} (2.58 S_{60\mu\text{m}} + S_{100\mu\text{m}}) \text{Wm}^{-2} \quad (2)$$

For the infrared selected galaxies in the *IRAS* 2 Jy sample, the mean value of  $q$  is  $\simeq 2.35$  (Yun, Reddy and Condon 2001). Given the FIR luminosity and radio flux density of IRAS 12032+1707, we estimate  $q = 1.77$ . This value appears low compared with the mean of 2.35 and could imply the presence of an AGN. This appears contradictory to the non-detection of a compact radio AGN core.

However, radio-excess objects in the *IRAS* 2 Jy sample are defined as those objects having a radio luminosity that is greater than 5 times larger than predicted by the radio-FIR correlation. Equivalently, this means objects for which  $q \leq 1.64$ . Furthermore, IRAS 12032+1707 has a very large infrared luminosity ( $\log(L_{\text{IR}}/L_{\odot}) = 12.57$ ), placing the galaxy at the high tail of the ULIRG luminosity distribution (Kim and Sanders 1998). For the most luminous sources in the *IRAS* 2 Jy sample, scattering from the radio-FIR correlation is significantly larger than for the weaker sources with weaker FIR flux densities. Therefore, the relatively low  $q$ -value for our source is not sufficient to indicate the presence of an AGN component. Other evidence that IRAS 12032+1707 is starburst-powered comes from its relatively cool IR color,  $F_{25\mu\text{m}}/F_{60\mu\text{m}} = 0.18$  (Kim and Sanders 1998). It is only for warm colors ( $F_{25\mu\text{m}}/F_{60\mu\text{m}} > 0.25$ ) that an AGN component is required to explain the resulting dust temperatures.

#### 4.2. IRAS 12032+1707 OH and HI

The zero-intensity line width of the OH maser emission in IRAS 12032+1707 is around  $2000 \text{ km s}^{-1}$ , which makes this source the host of one of the broadest OH megamaser lines. As mentioned in the introduction, this velocity range could be due to a combination of effects such as disk rotation and gas flows. Due to the limited SNR in our data, it is difficult to determine unambiguously the cause of the masers in IRAS 12032+1707. Below we discuss a few possible scenarios that could agree with our observations.

##### 4.2.1. Multiple disks

It has been suggested that very broad OH megamaser lines might be a combination of maser emission occurring in *both* of the merging nuclei, as is the case for the OH megamaser prototype Arp 220 (Diamond et al. 1989). We can rule out that maser emission in IRAS 12032+1707 is the combined emission from the southern and northern nuclei, since it is clear that all maser emission occurs only in the northern nucleus (Sect. 3.1).

We can not however exclude the possibility that the northern nucleus itself is made up of two more closely interacting galaxies. In Arp 220 the nuclei have a projected separation of only 300 pc,

which would correspond to an angular resolution of 86 mas at the distance of IRAS 12032+1707, much smaller than the near-infrared seeing limit of  $0.73''$  reported for the NIR image (Kim et al. 2002). This issue requires further investigation by future higher resolution infrared and optical imaging, combined with VLBI maser data.

In the OH megamaser source Mrk 231 HI absorption has been seen against a faint continuum disk (Carilli et al. 1998), and the HI velocity field displays a gradient in the same direction as the OH megamaser disk (Klöckner et al. 2003). In particular, the HI absorption velocities encompass those of the OH lines. Assuming that HI absorption in IRAS 12032+1707 has the same close correlation to OH as the HI in Mrk 231, then the fact that HI only partly covers the OH velocities implies that the HI absorption is seen against only one of the disks.

##### 4.2.2. A single nuclear disk

A clue to the nature of the OH maser emission must be given by the plot of the centroid position of the different velocity components. Clearly, there is a structured velocity field, with a bulk gradient in the north-south direction. If we assume that all maser emission belongs to a single disk-like structure, with a major axis going through the three most redshifted points at a position angle (PA) of  $11^\circ$  (Fig. 3), we can plot the data as velocity versus distance along this axis (Fig. 7). A least squares fit to the data points yields a gradient of  $55 \text{ km s}^{-1} \text{ pc}^{-1}$  over 17 pc. In total, this would mean an enclosed mass of  $2.2 \times 10^8 \sin^{-2} i M_{\odot}$  within a radius of 8.5 pc. Such a velocity gradient is surprisingly high given the gradients observed in other OH megamaser galaxies. For instance, for both III Zw 35 and Mrk 231, the velocity gradient is close to  $1.5 \text{ km s}^{-1} \text{ pc}^{-1}$  (Pihlström et al. 2001; Klöckner et al. 2003).

In contrast to the case of multiple disks suggested in Sect. 4.2.1, a scenario with a single disk for IRAS 12032+1707 makes it difficult to understand why the HI absorption covers only part of the OH velocity range (assuming that the HI and OH are parts of the same neutral gas structure).

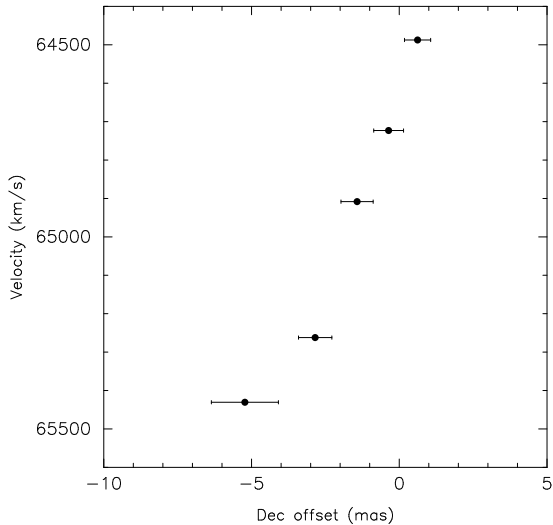


Fig. 7.— IRAS 12032+1707: Velocity plotted as a function of position along the axis delineated by the three redshifted components.

#### 4.2.3. A disk and an inflow

An alternative interpretation of Fig. 3 could include two different gas components. A couple of facts support the possibility of two physically different OH maser components in IRAS 12032+1707. Firstly, single-dish variability studies show that the two strongest and most blueshifted peaks have a variable flux density while the redshifted emission displays no significant variability (J. Darling, priv. comm). Secondly, the H I absorption velocities cover only the redshifted OH components (Sect. 3.3). If the H I has a common origin with the redshifted OH gas, the blueshifted and redshifted masers are likely to be physically different gas structures.

Studying the relative location of maser components in Fig. 3, we suggest that the two most blueshifted masers (which also are the brightest ones) could represent the tangent points of a circumnuclear disk. With an inclined disk (or torus), the tangent points will have the longest paths of velocity coherent gas, resulting in regions of very strong maser emission. This effect has been observed in III Zw 35 (Pihlström et al. 2001). The rotational velocity of such a torus or disk structure in IRAS 12032+1707 would be  $118 \sin^{-2}i \text{ km s}^{-1}$  at a radius of 3 pc, yielding a modest enclosed mass of  $5 \times 10^6 \sin^{-2}i M_{\odot}$ .

If the two blueshifted masers define the major axis of a disk component, the redshifted masers are directed more or less perpendicular to the disk (Fig. 3). By studying the optical and NIR images of IRAS 12032+1707 (Veilleux et al. 2002) it can be seen that the southern optical nucleus is located slightly west of south, with respect to the northern nucleus. Tentatively, the redshifted masers could arise in gas that has been disturbed by tidal interactions between the merging nuclei. With the caveat of over-interpreting our low SNR data, it is tantalizing to note that there is a weak hint in Fig. 7 of gas closer to the nucleus moving with higher velocity with respect to the nucleus, than does the gas further away.

In this scenario we suggest that the H I and the redshifted OH originate in the same gas component. Any gas associated with the H I absorption must thus necessarily be in front of the background continuum. Assuming the blue masers define a disk, it is plausible that the H I is seen in absorption against a weak radio continuum emitted by this disk. Given a limited field of view in the VLBA observations, in addition to an only tentative detection of the radio continuum, it is justified to question whether the radio continuum in fact coincides at all with the maser emission. We note that VLA A-array observations have showed that all radio continuum emission originates in the northern optical nucleus (J. Darling, priv. comm.), and the OH maser emission is located in the same region. Since H I absorption requires the presence of a background continuum, this is consistent with the H I absorption and OH masers occurring in the same region, at least on scales of a few kpc (corresponding to the VLA A-array resolution).

The optical systemic velocity of the nucleus is  $65055 \text{ km s}^{-1}$  with an  $1\sigma$  error of  $\pm 70 \text{ km s}^{-1}$  (Kim and Sanders 1998). Comparing the optical systemic velocity with the OH and H I velocities is hard since the optical redshift is measured for the whole IRAS 12032+1707 system, and thus does not separate the optical nuclei. In addition, the velocity is determined from optical emission lines that are often broad and might not properly reflect the systemic velocity since the emission lines may be associated with gas in motion with respect to the nucleus. Nevertheless, within a  $3\sigma$  limit the systemic velocity is consistent with redshifted maser components *falling in* towards the nucleus.

Veilleux et al. (1999) reports on optical emission lines in IRAS 12032+1707, that are broad compared to the typical ULIRG, consistent with the presence of an infalling gas component.

Neutral gas flows have been observed previously in other galaxies. For instance, VLA observations of the 1667, 1665 and 1612 MHz OH lines in the Galactic Center have revealed gas streaming inwards from the CNB (the CircumNuclear Disk) toward SgrA\* (Karlsson et al. 2003). The streamer can be seen over a velocity range of  $\sim 100$  km s<sup>-1</sup>. Furthermore, HI studies have extensively been used to trace merger dynamics, and one example is the detailed studies of HI emission in ‘The Antennae’. Hibbard et al. (2001) have mapped high HI column densities exceeding  $10^{22}$  cm<sup>-2</sup> in the region of the merging disks in this source. It is not unlikely that similar column densities could be probed by HI absorption in a merger like IRAS 12032+1707.

#### 4.3. IRAS 14070+0525

A major difficulty with interpreting the OH megamaser emission in IRAS 14070+0525 is that we only detect a fraction of the total single dish emission. As already mentioned, a reason why so much emission is resolved out may be the lack of short baselines in our VLBA observations. The offset between the two detected peaks is not significant. Optical and NIR imaging cannot distinguish more than one nucleus in IRAS 14070+0525, and this source is interpreted as a merger where the nuclei have more or less coalesced (Veilleux et al. 2002). Two nuclei could thus be located close to each other, and violent gas kinematics adding to the line width would be anticipated. More sensitive VLBI observations probing the emission on all spatial scales will be needed to gain a better understanding of the OH megamaser emission in this galaxy.

IRAS 14070+0525 is classified optically as a Seyfert 2 galaxy (Kim and Sanders 1998). However, the color given by  $F_{25\mu\text{m}}/F_{60\mu\text{m}}$  flux density ratio is only 0.13, and does not indicate the presence of an AGN. Contrary to IRAS 12032+1707, IRAS 14070+0525 falls on the radio-IR correlation with  $q = 2.4$  (Condon et al. 1998; Kim and Sanders 1998), and no compact radio emission associated with an AGN was detected. Hence, the radio emission is diffuse and consistent with a star-

burst. Given the low 1.4 GHz flux density of 5 mJy (Condon et al. 1998), a slightly resolved starburst would be expected to fall below our detection limit in these observations.

#### 5. Summarizing remarks

We have presented VLBA data on the broad OH megamaser emission in two IRAS galaxies IRAS 12032+1707 and IRAS 14070+0525. Due to insufficient coverage at short uv-spacings, only a minor part of the OH flux density was detected in the second source, IRAS 14070+0525. We find no significant evidence of an ordered velocity field in this source, but these results are inconclusive due to a very low SNR.

Almost all OH emission previously detected by single dish has been recovered in IRAS 12032+1707, and is found on a compact scale of  $< 100$  pc. The emission shows an ordered velocity field that could be consistent with a single disk. Although this may be the simplest explanation, we prefer an alternative explanation that better ties with the HI absorption data and variability studies of the maser emission. In this scenario, the two strongest and most blueshifted maser features would be the tangent points of a disk with major axis in the north-west to south-east direction. The remaining, redshifted maser features are aligned roughly perpendicular to this disk, extending to the south, i.e., the direction in which the second optical nucleus is located. This redshifted emission could thus be associated with tidally streaming gas falling onto the northern optical nucleus. The HI absorption covers the velocities of the redshifted maser emission, suggesting a common origin.

We note that this scenario is speculative given the number of data points. This should be confirmed with VLBI using a number of large dishes to increase the SNR. It would also be interesting to study high resolution CO data of this source. CO is known to be a good tracer of gas flows and disk structures in ULIRGs, and would thus give valuable information about the molecular gas dynamics.

#### 6. Acknowledgments

The National Radio Astronomy Observatory is a facility of the National Science Foundation operated under cooperative agreement by Associated

Universities, Inc. YMP wishes to acknowledge L.O. Sjouwerman, A.J. Mioduszewski and E.M.L. Humphreys for helpful comments on both the data reduction as well as on the interpretation.

## REFERENCES

- Alton, P.B., Davies, J.I., & Bianchi, S., 1999, *A&A*, 343, 51
- Baan, W. A., Wood, P. A. D., and Haschick, A. D. 1982, *ApJ*, 260, L49
- Baan, W. A., Haschick, A. D., & Henkel, C. 1989, *ApJ*, 346, 680
- Baan, W. A., Rhoads, J., Fisher, K., Altschuler, D. R., and Haschick, A. 1992, *ApJ*, 396, L99
- Baan, W. A., Salzer, J. J., and Lewinter, R. D. 1998, *ApJ* 509, 633
- Carilli, C. L., Wrobel, J. M., and Ulvestad, J. S. 1998, *AJ*, 115, 928
- Condon, J. J., Cotton, W. D., Greisen, E. W., Yin, Q. F., Perley, R. A., Taylor, G. B., and Broderick, J. J. 1998, *AJ*, 115, 1693
- Darling, J., and Giovanelli, R. 2001, *AJ*, 121, 1278
- Darling, J., and Giovanelli, R. 2002, *AJ*, 124, 100
- Diamond, P. J., Norris, R. P., Baan, W. A., and Booth, R. S. 1989, *ApJ*, 340, L49
- Diamond P. J., Lonsdale C. J., Lonsdale C. J., and Smith H. E. 1999, *ApJ*, 511, 178
- Heckman, T.M., Armus, L., & Miley, G.K., 1990, *ApJS*, 74, 833
- Helou G., Soifer B.T. & Rowan-Robinson M., 1985, *ApJ*, 298, L7
- Hibbard, J. E., van der Hulst, J. M, Barnes, J. E., & Rich, R. M., 2001, *AJ* 122, 2969
- Karlsson, R., Sjouwerman, L .O., Sandqvist, Aa., & Whiteoak, J.B., 2003, *A&A* 403, 1011
- Kim, D.-C., Veilleux, S., & Sanders, D. B. 2002, *ApJS*, 143, 277
- Kim, D.-C., and Sanders, D. B. 1998, *ApJS*, 119, 41
- Klöckner, H-R., Baan, W. A., and Garrett, M. A. 2003, *Nature*, 421, 821
- Klöckner, H-R. and Baan, W. A., 2004, *A&A*, 419, 887
- Martin, J. M., Le Squeren, A. M., Bottinelli, L., Gouguenheim, L., and Dennefeld, M. 1988, *A&A*, 202, 117
- Pihlström Y. M., Conway J. E., Booth R. S., Diamond P. J., and Polatidis A. G. 2001, *A&A* 377, 413
- Smith, H. E., Lonsdale, C. J., Lonsdale, C. J., and Diamond, P. J. 1998, *ApJL*, 493, L17
- Staveley-Smith L., Cohen R.J., Chapman J.M., Pointon L. & Unger S.W., 1987, *MNRAS*, 226, 689
- Veilleux, S., Kim, D.-C., and Sanders, D. B., 2002, *ApJS*, 143, 315
- Veilleux, S., Kim, D.-C., and Sanders, D. B. 1999, *ApJ*, 522, 113
- Yun, M. S., Reddy, N. A., & Condon, J. J., 2001, *ApJ*, 554, 803